J Polym Environ (2013) 21:303–311
DOI 10.1007/s10924-012-0523-5

ORIGINAL PAPER

Effect of Biaxial Stretching on Thermal Properties, Shrinkage and Mechanical Properties of Poly (Lactic Acid) Films

Jyh-Horng Wu · Ming-Shien Yen · Chien-Pang Wu · Chia-Hao Li · M. C. Kuo

Published online: 9 August 2012

Abstract This study produced poly (lactic acid) sheets using a biaxial stretching process, to investigate the effects of biaxial stretching on thermal properties, crystallinity, shrinkage and mechanical properties of PLA films. The results of differential scanning calorimetry show that the glass temperature peak of PLA films, which weakened after stretching. The cold crystallization peak of PLA films nearly disappeared at stretch ratios of 4×4 with a stretching rate above 50 %/s. The orientation and strain crystallization of PLA films were suppressed at stretching temperatures of approximately 100–110 °C. The shrinkage of PLA decreased proportionally to the stretch rate and inversely proportional to the stretching temperature, suggesting that the internal stresses frozen in the amorphous phase were an indication of a decrease in the crystallinity of the films, implying that PLA films would be best suited to low-shrinkage applications. The stress–strain of the PLA films increased considerably following the biaxial stretching process. In addition, PLA films exposed to hot water treatment show a slight decrease in stress values, probably attributable to a relaxation of the molecules, which have undergone orientation but failed to crystallize.

Keywords Poly (lactic acid) · Biaxially stretching · Shrinkage

J.-H. Wu · C.-P. Wu · C.-H. Li
Material Application Center, Industrial Technology Research Institute, Tainan City, Taiwan
e-mail: george6916@yahoo.com.tw

M.-S. Yen · M. C. Kuo (✉)
Department of Materials Engineering, Kun Shan University, No. 949, Da-Wan Rd., Yong-Kang Dist., Tainan City 71003, Taiwan, ROC
e-mail: muchen@mail.ksu.edu.tw

Introduction

Poly (lactic acid) (PLA) has recently been attracting a great deal of attention due to the fact that it can be produced using renewable resources. It can be found in applications, such as packaging [1, 2], engineering [3], textiles [4], automotive [5], biomedical [6–9] and tissue engineering [10, 11]. According to the specific requirements of individual applications, PLA can undergo conventional polymer processing techniques such as sheet extrusion, injection molding, thermoforming, blow molding, and fiber spinning [12]. It tends to crystallize very slowly, remaining amorphous even after polymer processing, causing a significant softening of PLA above the glass transition temperature (T_g) [13]. Ironically, the relatively low glass transition temperature and thermal stability of PLAs limits the number of potential applications to which it can be applied [14–19]. For this reason, researchers have proposed a variety of methods to enhance the physical properties of PLA, such as blending [18, 19], crosslinking [20–22], compositing [23–25], and processing [16, 26, 27].

As reported, the stretching processing is easy to enhance the physical properties in PLA products. It can be anticipated that increasing the crystallinity will have a positive influence on mechanical and thermal stability. In a previous study, Kokturk et al. [16] investigated the effects of uniaxially deforming PLA. Observing its influence on the development of crystalline structures. Smith et al. [26] reported a Raman technique to characterize the crystallinity and dimensional stability of PLA films. Yu et al. [27] studied the influence of annealing and orientation on microstructures and the mechanical properties of PLA. The objective of this study was to characterize the thermal properties, shrinkage and mechanical properties of PLA sheets, as influenced by biaxially stretching under various

conditions. This study also provides details on the mechanical properties of biaxially stretched PLA films following thermal treatment.

Experimental

Preparation of the Biaxially Stretched Films

The PLA (Wei Mon Industry Inc., Taiwan, grade: NCP0005) was extruded at temperatures ranging from 170 to 190 °C by a twin-screw (Werner and Pflederer, Model-ZSK 26 MEGA compounder) using a screw speed of 500 rpm extruded to form flat sheets 20 cm wide and 1 mm thick. From the sheets, 117 mm × 117 mm plates were cut. The plates were inserted into a biaxial film stretch machine (Bruckner, KARO IV) to prepare biaxially stretched films. The biaxial stretch ratios were 1–3 at stretch rate of 10–100 %/s. Stretching process was performed at 90–110 °C. All the specimens investigated in the present study were tabulated in Table 1.

Differential Scanning Calorimetry Analysis

Differential scanning calorimetry analysis (DSC) was performed using a TA apparatus (model No. Q2000). The weights of specimens used in the DSC scan are 4–5 mg. The test was first heated from 30 to 200 °C at a heating rate of 10 °C min^{-1} under nitrogen atmosphere. The degree of crystallinity (X_c) was determined from DSC analysis according to Eq. (1), where ΔH_c and ΔH_m are the cold crystallization enthalpy and melting enthalpy, respectively. An enthalpy of fusion (ΔH_m^o) of 93.6 J/g [28] was used for the perfectly crystalline PLA.

$$X_c = \frac{\Delta H_m - \Delta H_c}{\Delta H_m^o} \times 100 \quad (1)$$

Table 1 Experimental working conditions in this study

Sample no.	Temperature (°C)	Preheating time (s)	Stretching ratio (x)	Stretching rate (%/s)
1 (Unstretched PLA)	–	–	1 × 1	–
2	90	60	2 × 2	100
3	90	60	3 × 3	100
4	90	60	4 × 4	100
5	90	60	4 × 4	80
6	90	60	4 × 4	50
7	90	60	4 × 4	10
8	100	60	4 × 4	100
9	110	60	4 × 4	100

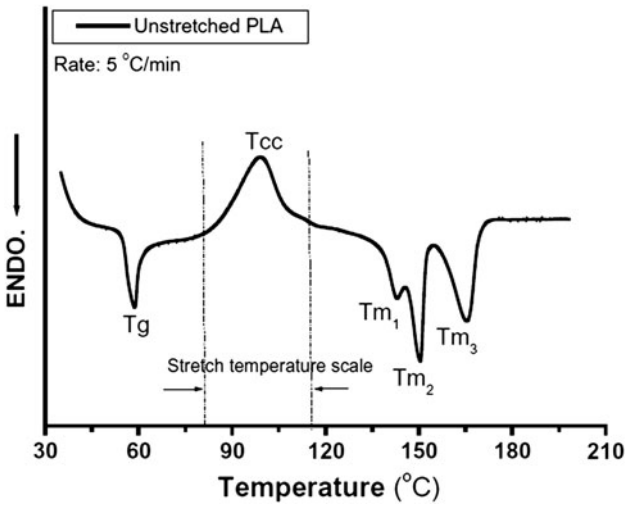

Fig. 1 DSC heating trace of unstretched PLA

X-ray Measurements

X-ray diffraction (XRD) measurements were conducted on a Rigaku D/Max RC X-ray diffractometer using CuK_α radiation ($\lambda = 1.5418$ Å) at 40 kV and 100 mA with a scanning rate of 2° min^{-1}.

Dynamic Mechanical Properties Analysis

Dynamic mechanical data were obtained using a dynamic mechanical analysis (DMA) instrument (TA Q800) with the following parameters: frequency 1 Hz, scan rate 3 °C/min and temperature range 30–120 °C.

Raman Spectroscopy Analysis

The Raman spectra were obtained using a Jasco Ventuno 21 (NRS-1000DT) system. The excitation source is a 532 nm laser for which power at the sample was reduced down to 0.3 mW.

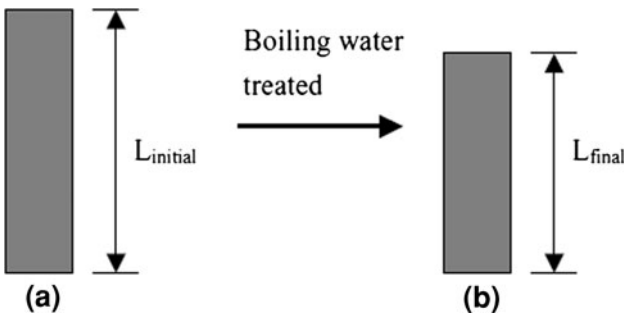

Scheme 1 Schematic showing stages in shrinkage: **a** original state with length $L_{initial}$; **b** state after immersion into the boiling water till no shrinkage change with length L_{final}

Table 2 DSC data of biaxially stretched PLA films

Sample no.	Thermal characteristics							
	ΔH_c (J/g)	ΔH_m (J/g)	T_g (°C)	T_{cc} (°C)	T_{m1} (°C)	T_{m2} (°C)	T_{m3} (°C)	X_c (%)
1	11.10	14.63	54.28	98.85	143.09	150.15	165.06	3.77
2	6.53	23.44	53.32	89.54	–	149.19	166.83	18.06
3	2.63	23.18	52.68	83.45	–	147.91	166.19	21.95
4	–	22.63	53.64	80.74	–	149.19	166.51	24.17
5	1.09	23.80	54.13	80.57	–	149.19	166.68	24.26
6	1.66	24.10	53.32	80.89	–	149.19	166.19	23.97
7	3.17	25.43	49.78	82.81	–	148.55	166.51	23.78
8	2.18	23.41	53.96	83.13	–	149.51	166.19	22.68
9	3.41	22.83	54.28	85.46	–	149.73	166.51	20.74

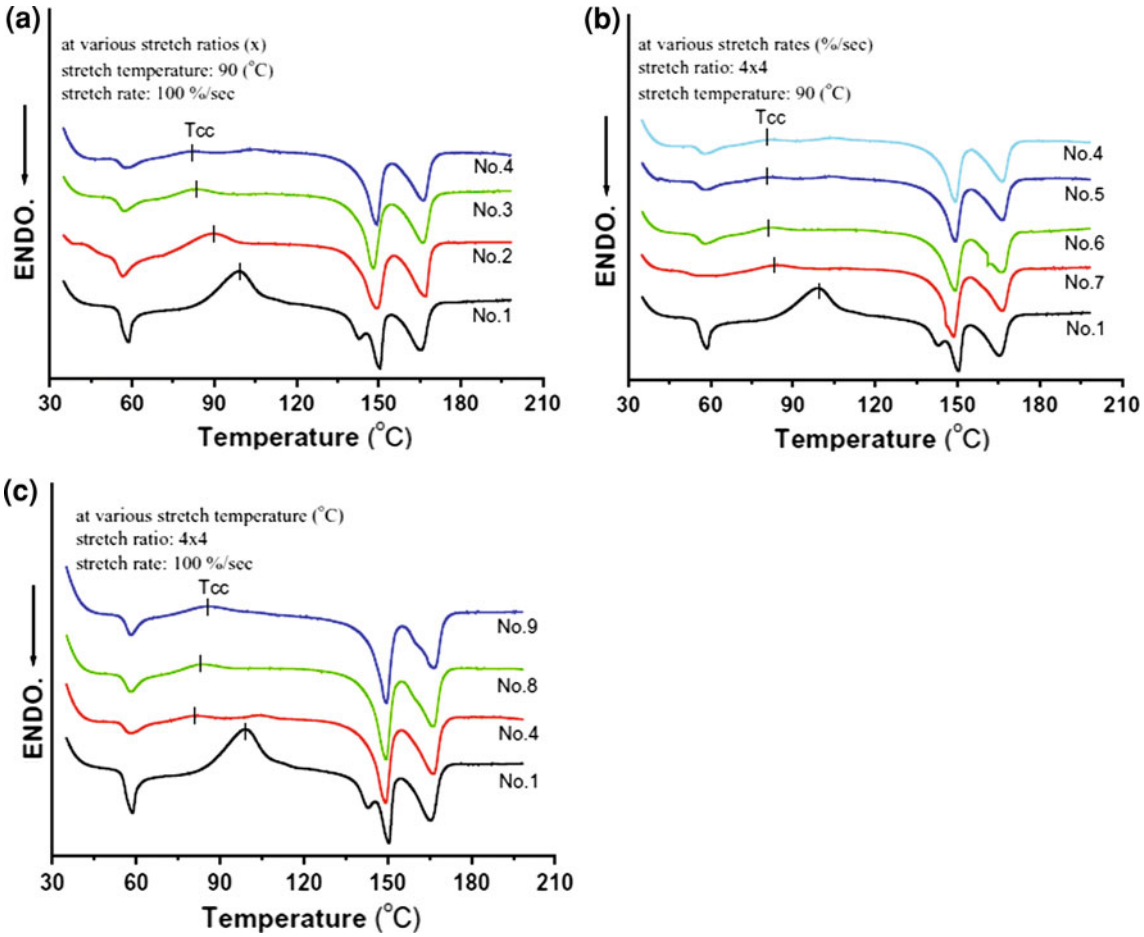

Fig. 2 DSC heating traces of PLA at various **a** stretching ratios, **b** stretching rates, **c** stretching temperatures

Shrinkage

The shrinkage of PLA films due to immersion into the boiling water till no shrinkage change was also measured, as represented in Scheme 1. The shrinkage percentage was calculated by the following equation:

$$\text{Shrinkage}\,(\%) = (L_{initial} - L_{final})/L_{initial}$$

where $L_{initial}$ and L_{final} are the length before and after boiling water treatment, respectively.

Mechanical Properties

The samples were determinant in the mechanical direction before and after biaxial stretching. Specimens used for

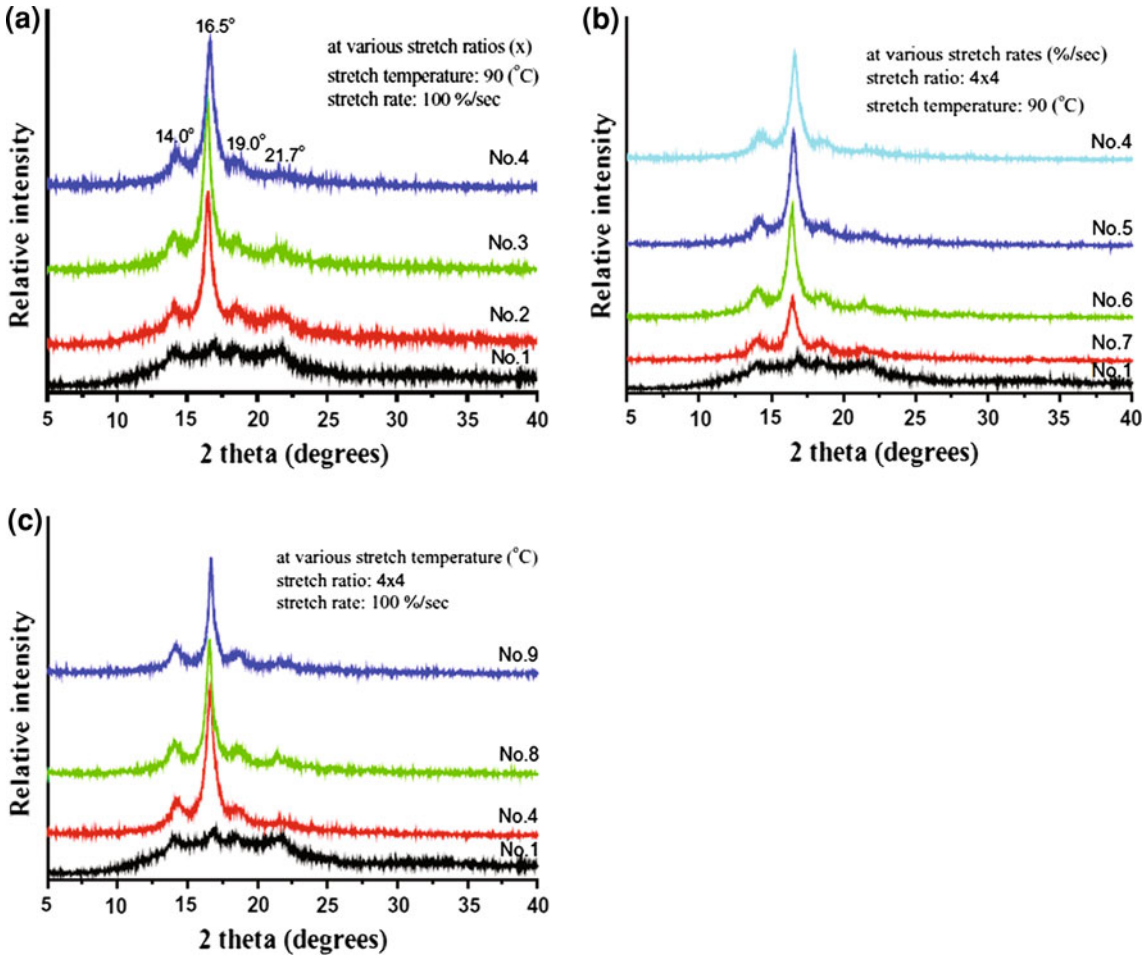

Fig. 3 XRD patterns of PLA at various **a** stretching ratios, **b** stretching rates, **c** stretching temperatures

tensile testing were cut from the stretched films according to ASTM D638 (5-mm width, and 50-mm length). Tensile tests were measured by a Universal Tensile Tester using a cross-head speed of 5 mm min^{-1} in compliance with the specifications of ASTM D638. In order to estimate the effect of thermal treat on the mechanical properties of the biaxially stretched PLA films, the unstretched and stretched PLA films were subjected to a hot-water treatment in a water bath at 90 °C for 10 min.

Results and Discussion

Thermal Properties

Figure 1 presents the results of DSC of unstretched PLA. The glass transition temperature (T_g), cold crystallization temperature (T_{cc}), and melting temperatures (T_{m1}, T_{m2} and T_{m3}) can be clearly observed in the curve. The thermal characteristics of PLA films are summarized in Table 2. It should be noted that three peaks could be observed in the melting of PLA. One possible explanation for the peaks is the melting of a proportion of the original crystals (T_{m2} and T_{m3}) [16] and the melting of crystals formed through a melt-recrystallization process (T_{m1}) [29–32] observed during a heating scan, respectively. In this study, we attempted to stretch PLA sheets at 90–110 °C using a stretching machine. Below 90 °C, elevated stress levels proved to be an impediment to the effective stretching of the material, and above 110 °C, the sheets became too sticky to be stretched uniformly. Between 90 and 110 °C, we succeeded in stretching the films biaxially to a ratio of 4 × 4.

Figure 2a shows the DSC curves and changes in T_g, T_{cc}, and T_m for PLA films stretched at 90 °C, according to a series of stretch ratios. Three changes were observed: (1) the cold crystallization peak shifted to a lower temperature with an increase in stretch ratio, nearly disappearing at stretch ratios of 4 × 4. This explains the reduction in the cold crystallization temperature and increase in crystallinity; (2) constraints imposed on the local structure were also reflected in the T_g peak, which weakened after stretching; and (3) the three-melting peaks transformed into double-melting peaks, which could be attributed to the transformation of imperfect crystals into perfect crystals during the

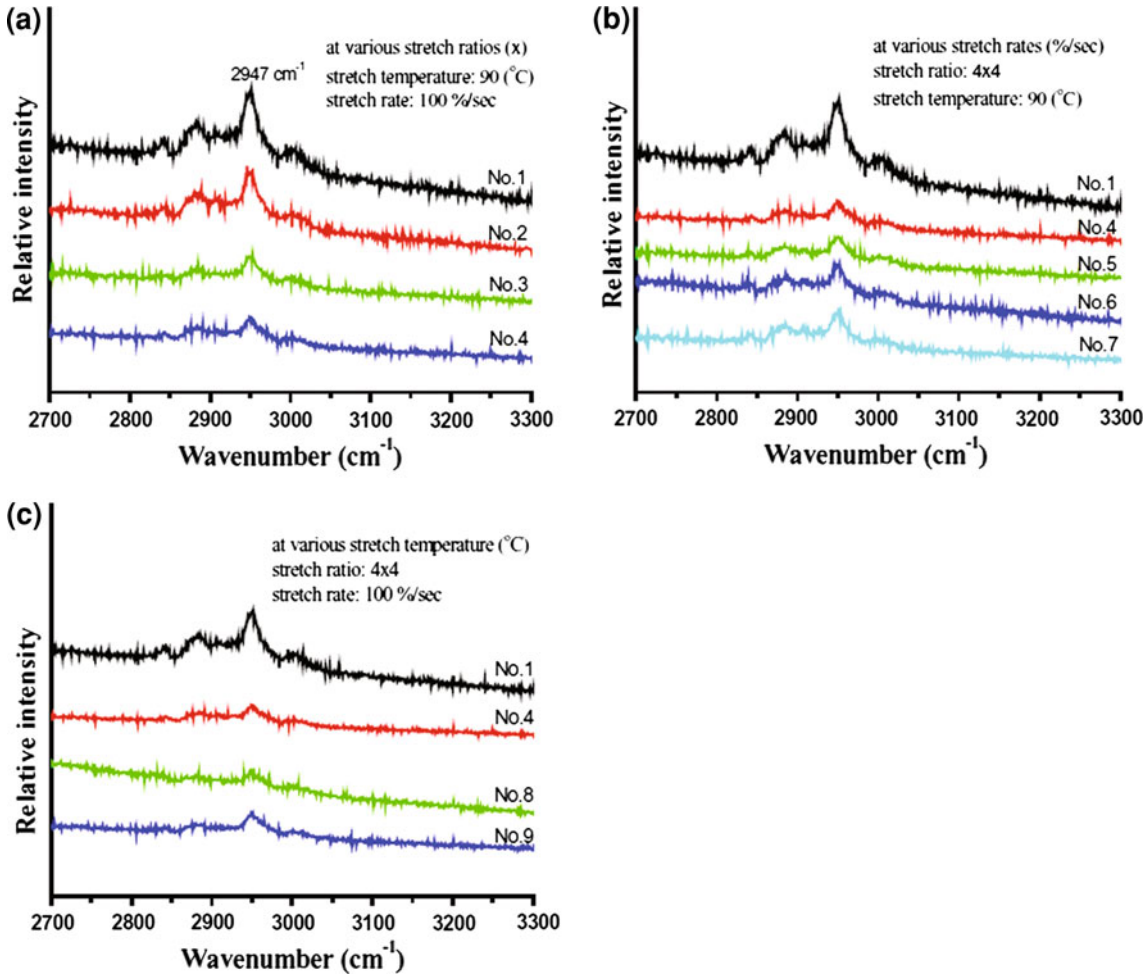

Fig. 4 Raman spectra of PLA at various **a** stretching ratios, **b** stretching rates, **c** stretching temperatures

biaxial stretching process. Further variations in the stretching rates of PLA films are shown in Fig. 2b. At a stretching rate at 10–50 %/s, cold crystallization peaks still exist in the curves. This indicates that stretching PLA films does not induce complete crystallization at low stretching rates. With an increase in the stretching rate above 50 %/s, the cold crystallization peak is barely noticeable in the curves. Figure 2c shows the DSC curves of PLA films stretched at various temperatures. The cold crystallization temperature shifted to a higher temperature with an increase in stretching temperature. This phenomenon could be attributed to the movement of the amorphous chains suppressing the orientation of molecules associated with crystallization.

XRD Analysis

Figure 3 displays the XRD patterns of PLA at various (a) stretching ratios, (b) stretching rates, and (c) stretching temperatures. Less intense peaks at $2\theta = 14.0°$, 16.5°, 19.0°, and 21.7° were found on the XRD patterns of the unstretched PLA (sample 1). According to the literature [33–35], these diffraction peaks can be assigned to the α-form of PLA (orthorhombic unit cell). Figure 3a and b show that the diffraction intensity of $2\theta = 16.5°$ increased at various stretching ratios and stretching rates, respectively. These results are associated with an obvious increase in the crystallinity of the films. Conversely, Fig. 3c shows that the diffraction intensity of $2\theta = 16.5°$ decreased as the stretching temperature increased. This indicates that the film does not induce crystallization easily at higher stretching temperatures.

Raman Analysis

The Raman spectra of PLA at various (a) stretching ratios, (b) stretching rates, and (c) stretching temperatures are shown in Fig. 4. The frequency region at 2,800–3,100 cm^{-1} was used to characterize orientation in the amorphous component. The most intense peak of unstretched PLA (sample 1) is at 2,947 cm^{-1}, which is assigned to the CH_3 symmetric stretch. The methyl group in this polymer shows

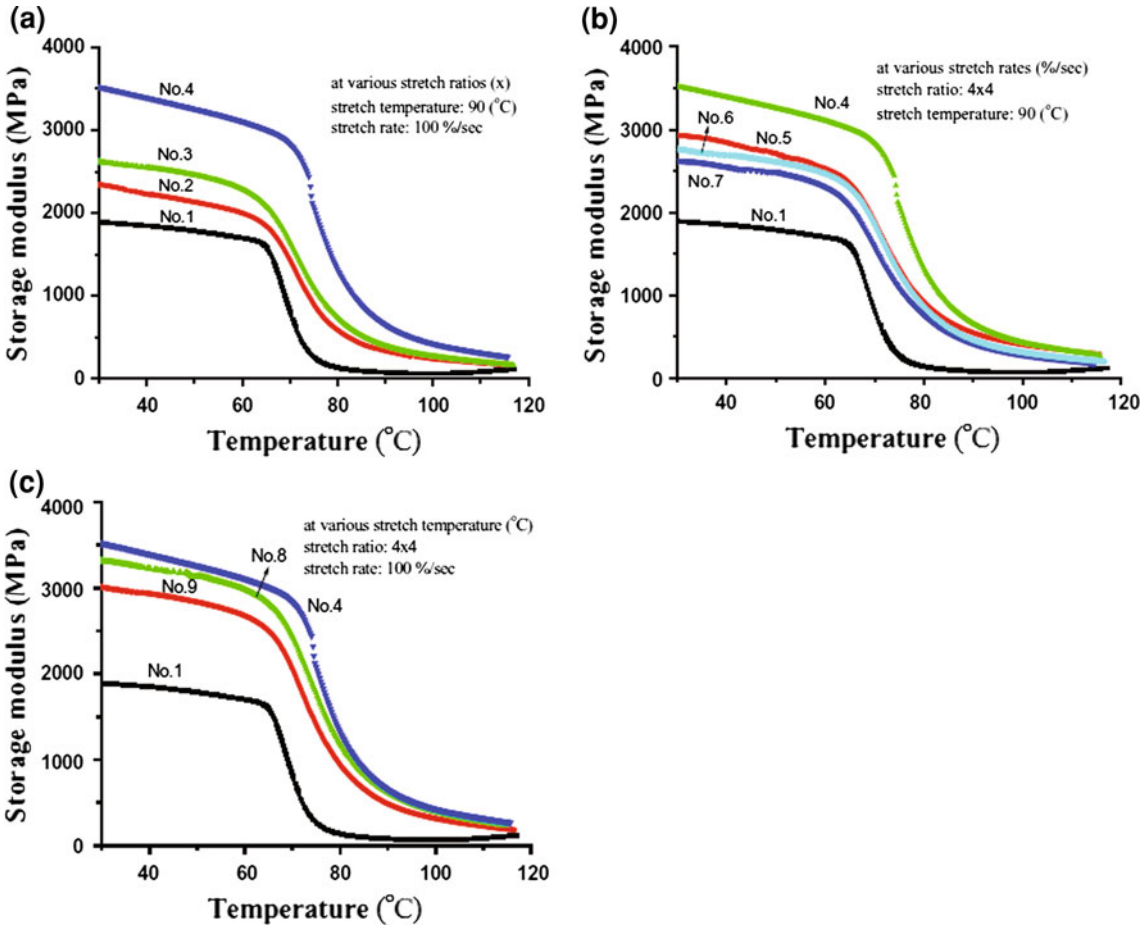

Fig. 5 Storage modulus of PLA at various **a** stretching ratios, **b** stretching rates, **c** stretching temperatures

the unique asymmetric stretching vibration at 3,000 cm^{-1} and symmetric stretching at 2,881 cm^{-1} [36]. Figure 4a and b show that the relative intensity for the 2,947 cm^{-1} band decreased as stretching ratios and stretching rates increased. These results are associated with an obvious increase in the molecular orientation of the films. Inversely, Fig. 4c shows that the relative intensity for the 2,947 cm^{-1} band increased in conjunction with stretching temperatures. This indicates that a polymer chains does not achieve easy orientation at higher stretching temperatures.

Dynamic Mechanical Properties

Figure 5 plots the storage modulus as a function of temperature for PLA at various (a) stretching ratios, (b) stretching rates, and (c) stretching temperatures. The storage modulus of the unstretched PLA (sample 1) decreased sharply at approximately 65 °C (namely glass transition temperature). An increase in temperature, gradually raised the storage modulus at approximately 105 °C (cold crystallization occurred at this temperature) [37–39]. Figure 5a and b show that the storage modulus of the biaxially stretched PLA films increased significantly in conjunction with stretching ratios and stretching rates. Conversely, Fig. 4c shows that the storage modulus of biaxially stretched PLA films decreased with increasing stretching temperatures. These results are consistent with those of the XRD and Raman experiment.

Mechanical Properties

The stress–strain curves of the films obtained under various processing conditions before and after hot water treatment are respectively shown as (a) and (b), in Figs 6, 7 and 8. Overall, the stress–strain value of PLA films increases considerably as a function of the stretching process. Zhang et al. [40] studies on biaxially stretched polystyrene showed a similar increase in the stress–strain. Figure 6a shows an increase in the stress value and a decrease in the strain value proportional to the degree of stretching induced. As show in Fig. 6b, unstretched PLA showed a slight increase in the stress value, but the strain value decreased obviously from 10.3 to 3.5 % (sample 1). This could be attributed to the hot water inducing cold

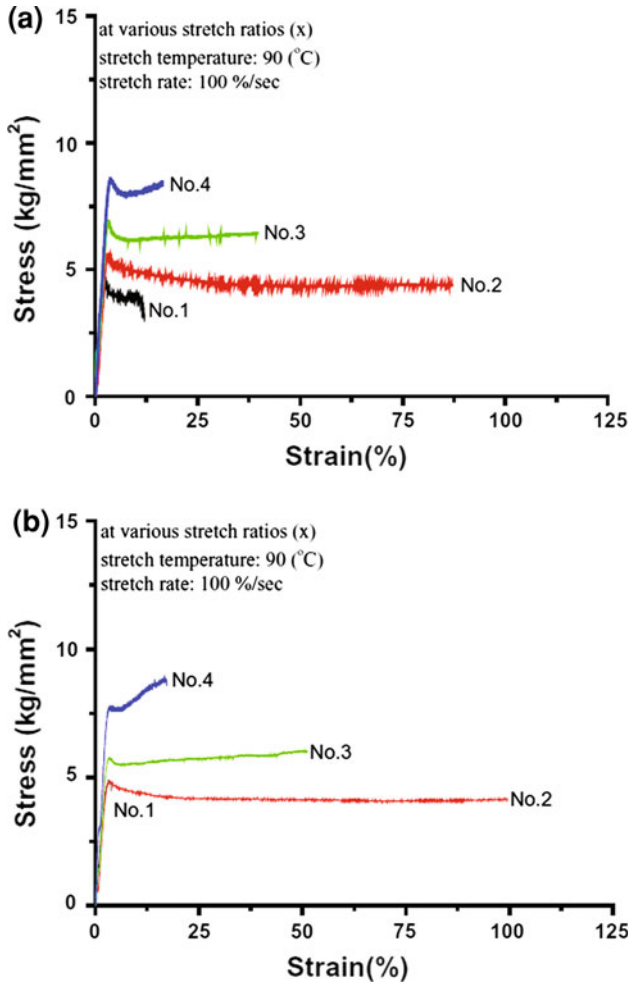

Fig. 6 Stress-strain curves of biaxially stretched PLA films at various stretching ratios. Plots **a** and **b** are before and after hot-water treatment of the PLA films, respectively

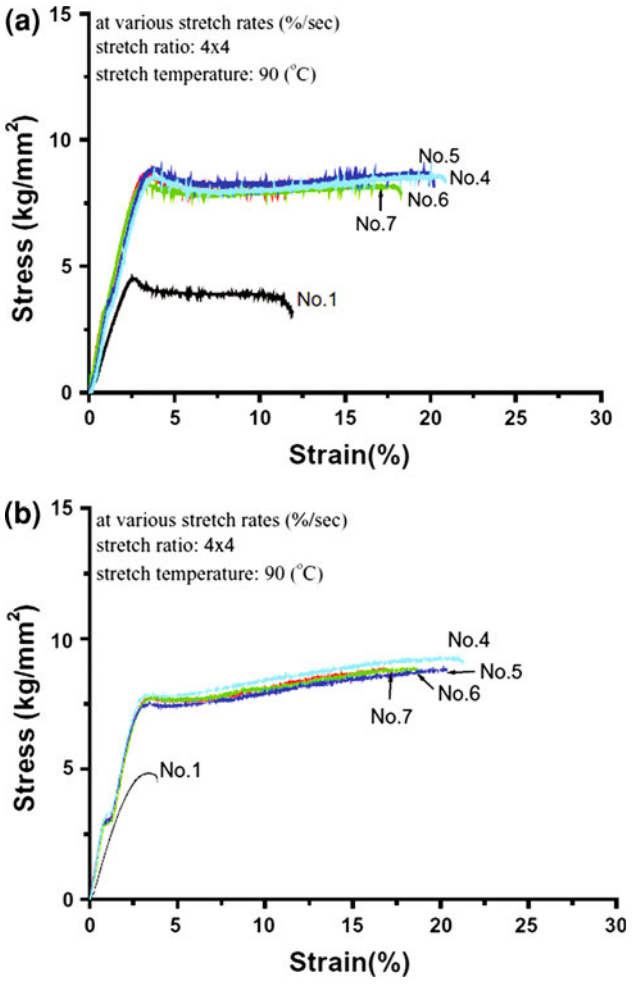

Fig. 7 Stress-strain curves of biaxially stretched PLA films at various stretching rates. Plots **a** and **b** are before and after hot-water treatment of the PLA films, respectively

crystallization of unstretched PLA, leading to a product with a higher degree of rigidity. Conversely, the stress value of stretched PLA decreased slightly, but the strain value increased from 16.1 to 17.5 % (sample 4), 39.8 to 51.3 % (sample 3), and 86.8 to 99.6 % (sample 2). This suggests that the oriented but uncrystallized molecules have a tendency to relax. Figure 7a shows that the variations in the stress values of biaxially stretched films are not obvious with an increase in stretching rate, but the strain values clearly increase. These results could be attributed to an increase in the orientation of the amorphous phase. Figure 7b shows that the stress value of biaxially stretched PLA decreased slightly, with a slight increase in strain value, when the films underwent hot water treatment. Figure 8a shows a decrease in the stress value of biaxially stretched films, but a slight increase in the strain value following an increase in stretching temperature. These results are associated with the active movement of the amorphous chains suppressing the orientation associated with crystallization. These results are consistent with the thermal properties shown in Fig. 2c. As show in Fig. 8b, treatment with hot water caused a slight decrease in stress value, and an inconspicuous change in the strain value.

Shrinkage

The principal molecular event responsible for the shrinkage is the increase of the internal energy (internal stresses) of the oriented system. This can be brought about by an increase in the temperature. Shrinkage affected for the first reason is called thermal or thermally stimulated shrinkage [41].

According to the DSC results, a biaxial stretching process produces PLA films with amorphous phase orientation and strain-induced crystallinity. Shrinkage must be minimized when films are heat-sealed to prevent the seal from puckering. Characterization of biaxially stretched films could provide highly valuable insights into the application

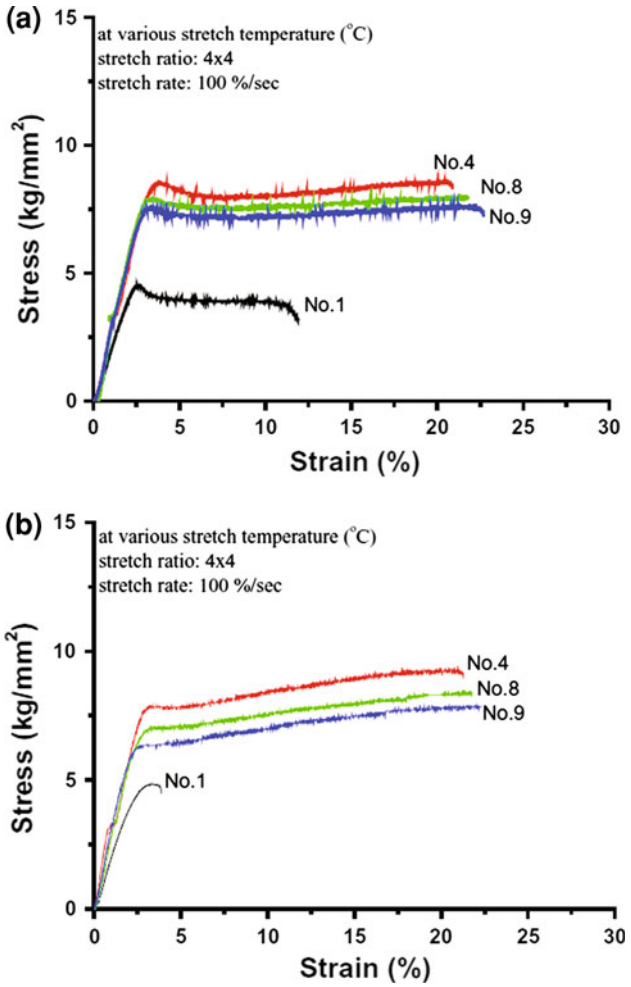

Fig. 8 Stress-strain curves of biaxially stretched PLA films at various stretching temperatures. Plots **a** and **b** are before and after hot-water treatment of the PLA films, respectively

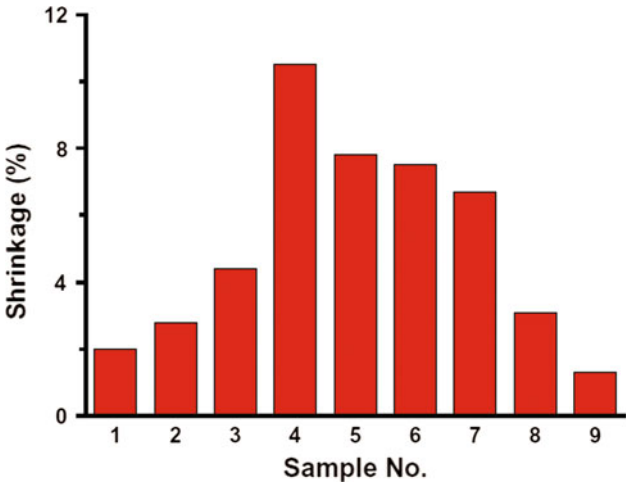

Fig. 9 Shrinkage of biaxially stretched PLA films

of PLA for food packaging. Figure 9 shows fluctuations in the shrinkage of PLA films under various conditions of biaxially stretching. The shrinkage was approximately 2 % for unstretched PLA (Sample 1). When the PLA was stretched, it exhibited an increase in shrinkage of 3–10 %, depending on the stretching ratio (Samples 2–4). This increase in shrinkage is a reflection of enhanced molecular orientation in the noncrystalline region and an increase in the internal stress frozen in the amorphous phase caused by an increase in stretching ratio. When heat sealing is performed at temperatures between below the crystalline melting point and above the glass-transition temperature (T_g) of PLA films, the oriented but uncrystallized molecules tend to coil up and relax producing the observed shrinkage. With a decrease in the stretching rate, the shrinkage in PLA (Sample 4) decreases to approximately 6.5–7.5 % (sample 5–7). This phenomenon can be attributed to a decrease in the internal stresses frozen in the amorphous phase of the films. With an increase in stretching temperature, the shrinkage of PLA (Sample 4) decreases to approximately 1–3.5 % (Samples 8 and 9). This decrease is a reflection of a decrease in the crystallinity and internal stresses in the film. These results are consistent with those related to the thermal properties of the material. Finally, the lower shrinkage of sample 9 relative to the sample 1, indicating an increased to the crystallinity and a decreased to thermal history of films that were plays the key role. Similar behavior was previously observed by Smith et al. [26], who proposed a model based on the molecular aspect of heat setting to reduce shrinkage in films. These observations suggest that PLA films are best suited to low-shrinkage applications.

Conclusion

The current study prepared a series of PLA films by biaxially stretching process. The thermal properties of PLA films showed a shift in the cold crystallization peak to a lower temperature following an increase in either stretching ratio or stretching rate. At stretching ratios of 4 × 4 and a stretching rate exceeding 50 %/s, the cold crystallization peak of PLA film nearly disappeared. The orientation associated with crystallization in PLA films was suppressed following an increase in stretching temperature. When heat sealing is performed at temperatures below the crystalline melting point and above the glass-transition temperature, PLA films exhibited oriented but uncrystallized molecules, which tended to coil up and relax, thereby producing shrinkage. The shrinkage of PLA decreased proportionally to the stretch rate and inversely proportional to the stretching temperature, suggesting the existence of internal stress frozen in the amorphous phase with a decrease in the crystallinity of the films. Furthermore, the mechanical properties of the PLA films increased

considerably after biaxial stretching. Following hot water treatment, PLA films showed a slight decrease in stress values, probably attributable to a relaxation of the molecules, which have undergone orientation but failed to crystallize.

References

1. Plackett DV, Holm VK, Johansen P, Ndoni S, Nielsen PV, Sipilainen-Malm T, Södergård A, Verstichel S (2006) Packag Technol Sci 19:1
2. Auras R, Harte B, Selke S (2005) Society of plastics engineers annual technical conference, vol 8, p 320
3. Choi YJ, Choung SK, Hong CM, Shin IS, Park SN, Hong SH, Park HK, Park YH, Son Y, Noh I (2005) J Biomed Mate Res Part A 75:824
4. Solarski S, Ferreira M, Devaux E, Fontaine G, Bachelet P, Bourbigot S, Delobel R, Coszach P, Murariu M, Ferreira ADS, Alexandre M, Degee P, Dubois P (2008) J Appl Polym Sci 109:841
5. Harris AM, Lee EC (2006) Annual SPE automotive composites conference, vol 1, p 252
6. Singh S, Ray SS (2007) J Nanosci Nanotechnol 7:2596
7. Bendix D (1998) Polym Degrad Stabil 59:129
8. Sawalha H, Schroën K, Boom R (2008) J Appl Polym Sci 107:82
9. Pompe W, Worch H, Epple M, Friess W, Gelinsky M, Greil P, Hempel U, Scharnweber D, Schulte K (2003) Mater Sci Eng A Struct Mater Prop Microstruct Process 362:40
10. Huang L, Zhuang X, Hu J, Lang L, Zhang P, Wang Y, Chen X, Wei Y, Jing X (2008) Biomacromolecules 9:850
11. Boccaccini AR, Notingher I, Maquet V, Jérôme R (2003) J Mater Sci-Mater Med 14:443
12. Schmack G, Tandler B, Vogel R, Beyreuther R, Jacobsen S, Fritz HG (1999) J Appl Polym Sci 73:2785
13. Celli A, Scandola M (1992) Polymer 33:2699
14. Perego G, Cella GD, Bastioli C (1996) J Appl Polym Sci 59:37
15. Ghosh S, Viana JC, Reis RL, Mano JF (2007) Polym Eng Sci 47:1141
16. Kokturk G, Serhatkulu TF, Cakmak M, Piskin E (2002) Polym Eng Sci 42:1619
17. Ikada Y, Tsuji H (2000) Macromol Rapid Commun 21:117
18. Tsuji H, Fukui I (2003) Polymer 44:2891
19. Ni C, Luo R, Xu K, Chen GQ (2009) J Appl Polym Sci 111:1720
20. Mitomo H, Kaned A, Quynh TM, Nagasawa N, Yoshii F (2005) Polymer 46:4695
21. Nijienhuis AJ, Grijpma DW, Pennings A (1996) J Polymer 37:2783
22. Suhartini M, Mitomo H, Nagasawa N, Yoshii F, Kume T (2003) J Appl Polym Sci 88:2238
23. Su Z, Liu Y, Guo W, Li Q, Wu C (2009) J Macromol Sci Part B Phys 48:670
24. Cao D, Wu L (1045) J Appl Polym Sci 2009:111
25. Hongbo L, Michel AH (2007) Polymer 48:6855
26. Smith PB, Leugers A, Kang S, Hsu SL, Yang X (2001) J Appl Polym Sci 82:2497
27. Yu L, Liu H, Xie F, Chen L, Li X (2008) Polym Eng Sci 48:634
28. Huang JW, Hung YC, Wen YL, Kang CC (2009) J Appl Polym Sci 112:3149
29. Yasuniwa M, Tsubakihara S, Sugimoto Y, Nakafuku C (2004) J Macromol Sci Part B Phys 42:25
30. Yasuniwa M, Satou T (2002) J Macromol Sci Part B Phys 40:2411
31. Yasuniwa M, Tsubakihara S, Satou T, Iura K (2005) J Macromol Sci Part B Phys 43:2039
32. Yasuniwa M, Tsubakihara S, Ohoshita K, Tokudome S (2005) J Macromol Sci Part B Phys 2001:39
33. Ikada Y, Jamshidi K, Tsuji H, Hyon SH (1987) Macromolecules 20:904
34. De Santis P, Kovacs A (1968) J Biopolymers 6:299
35. Hergeth WD, Lebek W, Stettin E, Witkowski K, Schmutzler K (1992) Makromol Chem 193:1607
36. Qin D, Kean RT (1998) Appl Spectrosc 52:488
37. Yeh JT, Huang CY, Chai WI, Chen KN (2009) J Appl Polym Sci 112:2757
38. Ke T, Sun X (2001) J Appl Polym Sci 81:3069
39. Martino VP, Jime'nez A, Ruseckaite RA (2009) J Appl Polym Sci 112:2010
40. Xiaomin Z, Abdellah A (2001) J Appl Polym Sci 82:2497
41. Trznadel M, Kryszewski M (1992) JMS Rev Macromol Chem Phys C32(3&4):259